

# PREDICTING SHAPE DEVELOPMENT: A RIEMANNIAN METHOD

*Doğa Türkseven\**

*Islem Rekik<sup>\*,†</sup>*

*Christoph von Tycowicz<sup>†</sup>*

*Martin Hanik<sup>†</sup>*

\* BASIRA Lab, Istanbul Technical University, Istanbul, Turkey

† Computing, Imperial-X Translation and Innovation Hub, Imperial College London, London, UK

† Freie Universität Berlin, Berlin, Germany

## ABSTRACT

Predicting the future development of an anatomical shape from a single baseline is an important but difficult problem to solve. Research has shown that it should be tackled in curved shape spaces, as (e.g., disease-related) shape changes frequently expose nonlinear characteristics. We thus propose a novel prediction method that encodes the whole shape in a Riemannian shape space. It then learns a simple prediction technique that is founded on statistical hierarchical modelling of longitudinal training data. It is fully automatic, which makes it stand out in contrast to parameter-rich state-of-the-art methods. When applied to predict the future development of the shape of right hippocampi under Alzheimer’s disease, it outperforms deep learning supported variants and achieves results on par with state-of-the-art.

**Index Terms**— Shape development, Prediction, Regression, Riemannian manifold

## 1. INTRODUCTION

Shapes of anatomical structures are of considerable medical interest, and they are encountered particularly often in the analysis of medical images. Researchers have shown that they should be modelled as elements of curved manifolds—shape spaces—instead of ordinary Euclidean space [1]. It is therefore imperative to develop methods for such spaces when working on problems involving anatomical shapes.

A particularly interesting and relevant task is the prediction of the future development of a shape—“How will an anatomical structure look like after a certain amount of time has passed?” This question is of great interest as shapes of anatomical structures are often correlated with (states of) diseases; see, e.g., [1–3]. Predicting how a shape will develop in the future could thus play a significant role for diagnosis and prevention as well as aid the physician in his choice of treatment.

One important example is the relation between the shape of the hippocampus and Alzheimer’s disease, as previous studies have shown that the former can be used to discriminate between Alzheimer’s and normal aging [4]. Thus, if the longitudinal development of the hippocampus’ shape can

be predicted, better prognosis can be achieved; and with Alzheimer’s improved early diagnosis can have a serious positive impact [5].

In order to uncover developmental trends in populations, longitudinal studies that involve repeated observations of individuals over a period of time play an essential role. The variability in such data can be distinguished as cross-sectional (i.e., between individuals), and longitudinal (i.e., within a single individual over time). Clearly, the latter is highly correlated violating the independence assumption of common statistical tools like mean-variance analysis and regression, thus requiring inferential approaches that can disentangle cross-sectional and longitudinal effects. For shape-valued data, another challenge that warrants attention is that curved spaces lack a global system of coordinates. To be able to assess differences in longitudinal trends requires a notion of transport between tangent spaces to spatially align subject-specific trajectories. For manifold domains, *parallel transport* has been shown to provide highly consistent transports [3, 6] with improved sensitivity over other methods.

In order to assess longitudinal and cross-sectional shape variation jointly, hierarchical statistical models pose an adequate and very flexible framework [7]. In recent years, various generalizations of such models to manifold-valued data have been proposed based on probabilistic [8] as well as least-squares theoretic [9–11] formulations. These approaches account for the inherent interrelations by describing each subject with its own parametric spatio-temporal model—most prominently geodesics. Additionally, the subject-specific trends are assumed to be perturbations of a population-average trend, which is referred to as “fixed” effect and is often of primary interest.

Population-level analysis apart, a few studies have focused on shape development prediction *for individuals*. A deep learning pipeline for predicting longitudinal bone shape changes in the femur to diagnose knee osteoarthritis was introduced in [2]. This approach utilizes a spherical encoding to map a 3D point cloud of the bone into a 2D image. It thereby relies on the assumption that the femura are (approximately) star-shaped. While the proposed pipeline produces accurate predictions of future bone shape, anatomies in general (e.g., hippocampi) are not star-shaped prohibiting a spherical en-

coding. A further limitation of the method is that it needs 3 separate observations for its prediction—a requirement that strongly hinders early diagnosis.

A varifold-based learning approach for predicting infant cortical surface development has been proposed in [12]. The method uses regression on varifold representations [13] to learn typical shape changes and uses the latter to predict from a single baseline. Although the method partly uses the curved space of diffeomorphisms, it only employs it for pre- and post-processing. It further requires the user to set several data-dependent parameters as optimal as possible (i.e., 2 data-dependent kernel sizes, a weighting between terms in the loss of the regression, the concentration of time points, and the number of nearest neighbors to be considered in a nearest neighbor search), leading to a relatively high entry-barrier for users.

In this work, we propose a novel method based on hierarchical statistical modeling to predict shape evolution. Representing the latter as geodesics in shape space allows to learn from longitudinal samples while respecting within-subject correlations. After training on full trajectories, the prediction requires only a single shape making it applicable when only the baseline observation of the longitudinal development is given. Conceptually, our prediction is very simple as it only consists of a parallel translation of the initial velocity of the mean trend and a subsequent evaluation of a geodesic. Furthermore, no data-dependent parameters need to be set, which makes the method very user-friendly.

To validate our approach on a real world problem, we use it to predict the development of the shape of the right hippocampus under Alzheimer’s. To the best of our knowledge, this is the first approach that applies longitudinal statistical modelling to the prediction of shape developments from a single baseline. In comparison to state-of-the-art, we observe an increased fidelity of subject-specific geodesic trends and a competitive prediction performance. At the same time, our approach is based on population-average dynamics and conceptually simple, thus, providing a high degree of interpretability. Upon acceptance of the paper we will make our source code public in order to make our method easily accessible.

## 2. METHOD

### 2.1. Prediction Method

### 2.2. The Basics

We first recall necessary basics from Riemannian geometry and geometric statistics; a good reference on them is [1].

A Riemannian manifold is a differentiable manifold  $M$  together with a Riemannian metric  $\langle \cdot, \cdot \rangle_p$  that assigns a smoothly<sup>1</sup> varying scalar product to every tangent space

$T_p M$ . The metric also yields a (geodesic) distance function  $d$  on  $M$ . A further central object is the Levi-Civita connection  $\nabla$  of  $M$ . Given two vector fields  $X, Y$  on  $M$ , it is used to differentiate  $Y$  along  $X$ ; the result is again a vector field, which we denote by  $\nabla_X Y$ . With a connection one can define a geodesic  $\gamma$  as a curve without acceleration, i.e.,  $\nabla_{\gamma'} \gamma' = 0$ , where  $\gamma' := \frac{d}{dt} \gamma$ . It is a fundamental fact that each element of  $M$  has a so-called normal convex neighbourhood  $U$  in which any two points  $p, q \in U$  can be joined by a unique length-minimizing geodesic  $[0, 1] \ni t \mapsto \gamma(t; p, q)$  that does not leave  $U$ . Since it is the solution of a second order differential equation,  $p$  and  $\gamma'(0)$  determine  $\gamma$  completely. Indeed, for every  $p \in U$  there are the Riemannian exponential  $\exp_p : T_p M \rightarrow U$  and logarithm  $\log_p := \exp^{-1} : U \rightarrow T_p M$  with  $\exp(v) := q$  such that  $\gamma'(0; p, q) = v$  and  $\log_p(q) = \gamma'(0; p, q)$ .

A further important fact is that in a Riemannian manifold one usually cannot identify tangent spaces with each other. Therefore, tangent vectors must be transported explicitly along curves between points—the so-called parallel transport. This process depends on the chosen path; however, in  $U$  we can always transport along the geodesic that connects origin and destination. Therefore, whenever we speak of parallel-translating a vector  $v$  from some  $p \in U$  to  $q \in U$  the transport along the geodesic from  $p$  to  $q$  is meant; the resulting vector (which is in  $T_q M$ ) is denoted by  $\Pi_p^q(v)$ .

Whenever we work with data, means are of interest. Given  $q_1, \dots, q_n \in M$ , their Fréchet mean is the minimizer of the Fréchet variance  $F(p) := \sum_{i=1}^n d(p, q_i)^2$ .

Interestingly, the set of all geodesics  $G(U) := \{\gamma : [0, 1] \rightarrow U \mid \gamma \text{ geodesic}\}$  in  $U$  can also be given the structure of a Riemannian manifold imposing a functional-based Riemannian metric [10]. As a consequence, we can compute Fréchet means of geodesics in  $G(U)$  if they are sufficiently localized; we assume the latter throughout this work.

We are now ready to introduce our model for shape prediction, which we will use for hippocampi. For this let  $M$  be any shape space that is a Riemannian manifold and  $U \subseteq M$  a normal convex neighbourhood consisting of the shapes of interest to us. Given a shape  $p^* \in U$  observed at time  $t_0$  our goal is to predict its future form  $q^* \in U$  at time point  $t_1$ . For simplicity of exposition we assume in the following that  $t_0 = 0$  and  $t_1 = 1$ . This can always be achieved when the times are viewed relative to an interval that contains them.

Our fundamental assumption is that  $p^*$  develops along a geodesic through  $U$ , i.e., there is  $\gamma_{p^*} \in G(U)$  such that the longitudinal development of  $p^*$  at time  $t$  is given by  $\gamma_{p^*}(t)$ . Several works have shown that this is often an adequate choice when modeling shape developments in the medical context [1, 3]. Then, since geodesics are determined by their starting point and initial velocity, we need to find  $\gamma'_{p^*}(0)$ ; because then

$$q^* = \exp_{p^*}(\gamma'_{p^*}(0)). \quad (1)$$

In other words, to predict the development of *any* shape  $p^* \in$

<sup>1</sup>Whenever we say “smooth” we mean “infinitely often differentiable”.

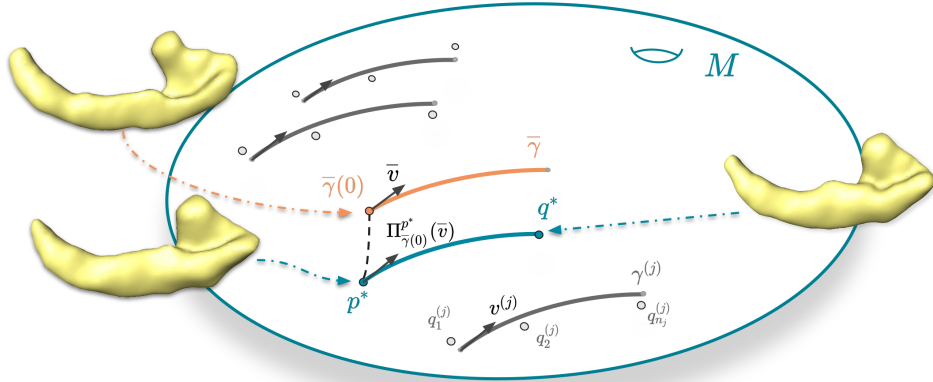


**Fig. 1.** Depiction of the shape prediction method in a shape space  $M$ . Examples of  $\bar{\gamma}(0)$ ,  $p^*$ , and  $q^*$  in the case of right hippocampi are shown in yellow.

$U$  that is of interest to us we need to approximate a vector field on  $U$  that encodes the direction and speed of change that  $p^*$  undergoes until time 1.

In the following, we propose an approach that infers this vector field from data. Assume  $N$  shapes similar to  $p^*$  (i.e., close to  $p^*$  in  $U$ ) from which we expect analogous progression are observed at a possibly varying number of time points, yielding (training) data  $(t_i^{(j)}, q_i^{(j)}) \in [0, 1] \times U$ , for  $i = 1, \dots, n_j$  and  $j = 1, \dots, N$ . Now, using geodesic regression [14] we can approximate the individual trajectories  $\gamma^{(1)}, \dots, \gamma^{(N)} \in G(U)$  of the training shapes. Utilizing the manifold structure of  $G(U)$  from [11], the (Fréchet) mean geodesic  $\bar{\gamma}$  of  $\gamma^{(1)}, \dots, \gamma^{(N)}$  can be computed. Note that  $\bar{\gamma}(0)$  and  $\bar{v} := \dot{\gamma}(0) \in T_{\bar{\gamma}(0)}M$  can be interpreted as the mean starting point and the average initial velocity of the trajectories of the training data, respectively. The geodesic  $\bar{\gamma}$  is further the central fixed effect that describes the data in a geodesic hierarchical model [9, 10].

The fact that the training shapes are close to  $p^*$  suggests that the parallel transport of  $\bar{v}$  to  $p^*$  is a good approximation of our target  $\gamma'_{p^*}(0)$ . We thus propose to use the approximation  $\gamma'_{p^*}(0) \approx \Pi_{\bar{\gamma}(0)}^{p^*}(\bar{v})$  in (1). Being a comparatively simple approach, our experiments show that it can be a very good choice. The process pipeline is shown in Fig. 1.

### 3. EXPERIMENTS

#### 3.1. Data and Methodology

**Dataset:** In order to evaluate our model we applied it to shape data of right hippocampi derived from 3D label fields provided by the Alzheimer’s Disease Neuroimaging Initiative (ADNI). The ADNI data base contains, amongst others, 1632 brain MRI scans with segmented hippocampi. From them, we assembled three distinct groups: subjects with Alzheimer’s

(AD), Mild Cognitive Impairment (MCI), and cognitive normal (CN) controls. The groups contained data from 80, 116, and 201 subjects, respectively; for each subject there were three MR images taken (approximately) six months apart. Correspondence of the surfaces (2280 vertices, 4556 triangles) was established in a fully automatic manner by registering extracted isosurfaces using the functional map-based approach of [15]. As the final preprocessing step, all meshes were aligned using generalized Procrustes analysis.

**Shape Space:** As shape space, we used the differential coordinate model (DCM) space from [16]. Working with triangular mesh representations it allows for explicit and fast computations.

**Comparison Methods:** The first comparison method was the varifold-based (Varifold) method from [12]. In order to test whether incorporating a deep neural network improves the prediction, we also tested the following variation of our proposed method: We tried both a generative adversarial network (GAN) and a cyclic GAN (cGAN) to learn a correction  $w_{p^*} \in T_{\bar{\gamma}(0)}M$  of  $\bar{v}$ . The idea was that shapes from different regions in  $U$  might show systematic differences in the direction into which they develop. Both the GAN and cGAN are designed to map the coordinate vector<sup>2</sup> of the cross-sectional difference  $[\log_{\bar{\gamma}(0)}(p^*)] \in \mathbb{R}^d$  to the correction vector  $[w_{p^*}] \in \mathbb{R}^d$ . They were trained on the baselines  $\{q_1^{(j)} \mid j = 1, \dots, N\}$  using 3-fold cross validation. The final prediction then became  $\gamma'_{p^*}(0) \approx \Pi_{\bar{\gamma}(0)}^{p^*}(\bar{v} + w_0)$  in (1).

In both the GAN and cGAN network, the generators consisted of four linear layers, with dropout layers and ReLU activation functions between them; the discriminators were composed of two linear layers without dropout. Both the GAN and cGAN used the sum of the binary cross entropy

<sup>2</sup>We denote the coordinate representation in  $\mathbb{R}^d$  of a tangent vector  $v$  w.r.t. a fixed but arbitrary basis by  $[v]$ .

Group	average mean vertex-wise error (MVE)					average geodesic distance (GD)	
	DCM	PDM	DCM+GAN	DCM+cGAN	Varifold	DCM	PDM
AD	<b>0.70 ± 0.02</b>	0.71 ± 0.02	0.73 ± 0.02	0.75 ± 0.02	<b>0.70 ± 0.07</b>	<b>15.60 ± 0.70</b>	37.50 ± 0.79
MCI	<b>0.64 ± 0.03</b>	<b>0.64 ± 0.03</b>	0.67 ± 0.03	0.75 ± 0.04	0.65 ± 0.07	<b>15.22 ± 1.01</b>	34.55 ± 1.81
CN	0.71 ± 0.09	0.72 ± 0.08	0.74 ± 0.07	0.80 ± 0.05	<b>0.70 ± 0.14</b>	<b>16.53 ± 1.89</b>	38.39 ± 4.44

**Table 1.** Comparison results for variants of our proposed method and the varifold-based prediction method. The best results in each group are bold (standard deviations only if they are also the smallest on the group).

and the difference  $\|\Pi_{\gamma^{(j)}(0)}^{\bar{\gamma}}(v^{(j)}) - \bar{v} - w_0\|_{\bar{\gamma}(0)}$  (with the norm that is induced by the Riemannian metric) as loss; for the cGAN the standard forward cycle consistency loss was also added. When referencing results obtained with the GAN and cGAN while using the DCM space as shape space, we use the notations (DCM+GAN) and (DCM+cGAN), respectively. To evaluate how important the DCM space is to the prediction, we also replaced it with the flat point distribution model (PDM) space from [17].

Finally, to further differentiate the behavior of our proposed and the varifold-based method we tested how well regressed geodesics in the DCM as well as the space of diffeomorphisms approximate the data. We report for all groups the averages of the mean vertex-wise error (MVE) between the vertices of the mesh belonging to  $\gamma^{(j)}(1)$  and the corresponding data mesh of  $q_3^{(j)}$  after rigid alignment.

**Software:** The computations in the DCM and PDM space were performed in Morphomatics v1.1 [18]. The GAN and cGAN were implemented in PyTorch. When training the them we used ADAM optimizer for both the generators and the discriminators. All computations involving varifolds were performed in Deformetrica 4.3.0rc0 [19].

**Parameter Settings:** For Varifold we used a smoothing kernel width of 20, a deformation kernel width of 15,  $t_0 = 0.5$ , concentration of time points of 1, and the number of points used from the cloud was set to 25. The GAN and cGAN used a probability of dropout of 0.2; learning rates of both the generators and discriminators were set to 0.0001. For each fold, we trained the network with 400 epochs. All parameters were determined through exploration.

**Evaluation Measures:** In order to assess the effectiveness of our model, we employed the MVE by calculating how much (after rigid alignment) each vertex deviates from its corresponding ground truth vertex. Moreover, to compare the DCM and PDM spaces we contrasted the MVE (which can be viewed as the intrinsic distance of the PDM space) with the geodesic distance  $d$  (GD) of the DCM space.

### 3.2. Results

The results of our prediction comparison are shown in Table 1. Even though the proposed method is a relatively simple approach, it not only performed better than GAN methods but was also faster and did not involve hyperparameter tuning. Also, differently structured GANs did not improve the

results by noticeable amount. Furthermore, we can see that using the DCM space is superior to using PDM space as its results are close w.r.t. MVE (the intrinsic PDM distance) but significantly worse w.r.t. the GD of the DCM space.

Group	average mean vertex-wise error (MVE)		
	AD	MCI	CN
DCM	<b>0.16 ± 0.06</b>	<b>0.17 ± 0.16</b>	<b>0.18 ± 0.18</b>
Varifold	0.68 ± 0.58	0.62 ± 0.47	0.73 ± 0.74

In comparison to the varifold-based approach, the proposed method achieves similar results, while always having smaller standard deviation. The results of the fitting tests between regression in DCM and the space of diffeomorphisms are shown in the inset above. Clearly, the approximation is superior when the DCM space is used, thus, demonstrating an improved fidelity of DCM geodesics over diffeomorphic representations.

## 4. CONCLUSION

In this paper, we proposed a novel method for predicting shape development based on hierarchical statistical modeling in Riemannian shape spaces. When applied to hippocampus shapes, our simple approach was more accurate and faster on its own than when deep learning-based approaches were added. Moreover, it produced results that were competitive to state-of-the-art while at the same time being more user-friendly and simpler—the latter assuring a high degree of interpretability. The method is thus a very good fit for shapes such as hippocampi whose development follows geodesics and that are well captured by population-average trends. As the latter assumption will not always be true, it is still a promising approach to incorporate deep learning: Whenever the development depends strongly on the individual characteristics of the baseline shape, we expect that deep learning methods can be used to find adjustments to our prediction (direction) that take the dependence into account. A path for future work is thus to test this hypothesis on further anatomical structures.

## 5. COMPLIANCE WITH ETHICAL STANDARDS

This research study was conducted retrospectively using human subject data made available in open access. Ethical ap-

proval was *not* required as confirmed by the license attached with the open access data.

## 6. ACKNOWLEDGMENTS

This work was partially funded by grants from the European H2020 Marie Skłodowska-Curie action (grant no. 101003403) and the Scientific and Technological Research Council of Turkey under the TUBITAK 2232 Fellowship for Outstanding Researchers (no. 118C288)<sup>3</sup>. We are grateful for the funding by DFG<sup>4</sup> and BMBF<sup>5</sup> as well as for the provision of the data set by the ADNI<sup>6</sup>.

## 7. REFERENCES

- [1] X. Pennec, S. Sommer, and P. T. Fletcher, Eds., *Riemannian Geometric Statistics in Medical Image Analysis*, Academic Press, London, 2020.
- [2] F. Calivá, S. Kamat, and A. M. Martinez et al., “Surface spherical encoding and contrastive learning for virtual bone shape aging,” *Med. Image Anal.*, vol. 77, pp. 102388, 2022.
- [3] E. Nava-Yazdani, H.-C. Hege, T. J. Sullivan, and C. von Tycowicz, “Geodesic analysis in Kendall’s shape space with epidemiological applications,” *J. Math. Imaging Vis.*, vol. 60, pp. 549–559, 2020.
- [4] E. Gerardin, G. Chételat, and M. Chupin et al., “Multidimensional classification of hippocampal shape features discriminates Alzheimer’s disease and mild cognitive impairment from normal aging,” *NeuroImage*, vol. 47, no. 4, pp. 1476–1486, 2009.
- [5] J. Rasmussen and H. Langerman, “Alzheimer’s disease - why we need early diagnosis,” *Degenerative Neurological and Neuromuscular Disease*, vol. 9, pp. 123–130, 2019.
- [6] M. Lorenzi and X. Pennec, “Geodesics, parallel transport & one-parameter subgroups for diffeomorphic image registration,” *Int. J. Comput. Vis.*, vol. 105, no. 2, pp. 111–127, 2013.
- [7] G. Gerig, J. Fishbaugh, and N. Sadeghi, “Longitudinal modeling of appearance and shape and its potential for clinical use,” *Med. Image Anal.*, vol. 33, pp. 114–121, 2016.
- [8] A. Bône, O. Colliot, and S. Durrleman, “Learning the spatiotemporal variability in longitudinal shape data sets,” *Int. J. Comput. Vis.*, vol. 128, no. 12, pp. 2873–2896, 2020.
- [9] P. Muralidharan and P. T. Fletcher, “Sasaki metrics for analysis of longitudinal data on manifolds,” in *Proceedings of the 2012 IEEE Conference on Computer Vision and Pattern Recognition*. 2012, pp. 1027–1034, IEEE.
- [10] E. Nava-Yazdani, H.-C. Hege, and C. von Tycowicz, “A hierarchical geodesic model for longitudinal analysis on manifolds,” *J. Math. Imaging Vis.*, vol. 64, no. 4, pp. 395–407, 2022.
- [11] M. Hanik, H.-C. Hege, and C. von Tycowicz, “A non-linear hierarchical model for longitudinal data on manifolds,” in *2022 IEEE 19th International Symposium on Biomedical Imaging (ISBI)*. IEEE, 2022, pp. 1–5.
- [12] I. Rekik, G. Li, W. Lin, and D. Shen, “Predicting infant cortical surface development using a 4d varifold-based learning framework and local topography-based shape morphing,” *Med. Image Anal.*, vol. 28, pp. 1–12, 2016.
- [13] J. Fishbaugh, S. Durrleman, M. Prastawa, and G. Gerig, “Geodesic shape regression with multiple geometries and sparse parameters,” *Med. Image Anal.*, vol. 39, pp. 1–17, 2017.
- [14] P. T. Fletcher, “Geodesic regression and the theory of least squares on Riemannian manifolds,” *Int. J. Comput. Vis.*, vol. 105, no. 2, pp. 171–185, 2013.
- [15] D. Ezuz and M. Ben-Chen, “Deblurring and denoising of maps between shapes,” *Comput. Graph. Forum*, vol. 36, no. 5, pp. 165–174, 2017.
- [16] C. von Tycowicz, F. Ambellan, A. Mukhopadhyay, and S. Zachow, “An efficient Riemannian statistical shape model using differential coordinates,” *Med. Image Anal.*, vol. 43, pp. 1–9, 2018.
- [17] T. F. Cootes, C. J. Taylor, D. H. Cooper, and J. Graham, “Active shape models-their training and application,” *Comput. Vis. Image Underst.*, vol. 61, no. 1, pp. 38–59, 1995.
- [18] F. Ambellan, M. Hanik, and C. von Tycowicz, “Morphomatics: Geometric morphometrics in non-Euclidean shape spaces,” 2021, <https://morphomatics.github.io/>.
- [19] A. Bône, M. Louis, B. Martin, and S. Durrleman, “Deformetrica 4: an open-source software for statistical shape analysis,” in *International Workshop on Shape in Medical Imaging*. Springer, 2018, pp. 3–13.

<sup>3</sup><https://basira-lab.com/normnets/> & <https://basira-lab.com/reprime/>

<sup>4</sup>Deutsche Forschungsgemeinschaft (DFG) through Germany’s Excellence Strategy – The Berlin Mathematics Research Center MATH+ (EXC-2046/1, project ID: 390685689)

<sup>5</sup>Bundesministerium für Bildung und Forschung (BMBF) through BIFOLD - The Berlin Institute for the Foundations of Learning and Data (ref. 01IS18025A and ref 01IS18037A)

<sup>6</sup>adni.loni.usc.edu